Persistent MgB_2 joints for react and wind magnets

OPEN ACCESS
IOP Publishing
Superconductor Science and Technology
Supercond. Sci. Technol. **37** (2024) 015009 (9pp)
https://doi.org/10.1088/1361-6668/ad06c3

Persistent MgB_2 joints for react and wind magnets

M Guven[1], P Zagura[1,*], C M Barker[1], M N Kutukcu[2], S Atamert[2], C R M Grovenor[1] and S C Speller[1]

[1] Department of Materials, University of Oxford, Parks Road, Oxford, OX1 3PH Oxford, United Kingdom
[2] EPOCH Wires Ltd, Unit 8, Burlington Park, Foxton, CB22 6SA Cambridge, United Kingdom

E-mail: petr.zagura@materials.ox.ac.uk

Received 20 July 2023, revised 12 October 2023
Accepted for publication 25 October 2023
Published 5 December 2023

Abstract

Ultra-low resistance joints are a key technology enabling superconducting magnets to operate in persistent mode and to achieve the temporal stability required for nuclear magnetic resonance and magnetic resonance imaging (MRI) applications. High performance superconducting joints are manufactured routinely for Nb–Ti and Nb_3Sn magnets, but technologies for joining other technological superconductors are still in the early stages of development. Here we report the use of a simple cold pressing and heat treatment procedure to fabricate persistent MgB_2 joints with resistance values $<10^{-12}$ Ω between MgB_2 wires that have already undergone the full wire reaction process. Trapped persistent currents of 172 A and 160 A were achieved under self-field and 1 T background field conditions respectively at a temperature of 20 K. This corresponds to a critical current ratio of 78% under these conditions, outperforming previously reported joints using fully reacted MgB_2 wire. These findings are relevant for the development of commercial MRI magnets with MgB_2 wires utilizing react and wind methods.

Supplementary material for this article is available online

Keywords: applied superconductivity, superconducting joints, magnesium diboride

1. Introduction

Superconducting materials are critical for a range of applications that affect daily life, and one of the most familiar of these is medical magnetic resonance imaging (MRI) that requires very stable fields to be generated in large magnets. Segmented coils are a common feature in the design of most MRI systems, leading to the requirement for wire-to-wire joints [1]. As a result, superconducting joints are a crucial component of magnets for MRI applications. A total circuit resistance $<10^{-12}$ Ω [2] is required to generate an ultra-stable magnetic field with a degradation rate of less than 0.1 $ppmh^{-1}$ [3]. While the technology to manufacture persistent mode joints is well known for wires of several of the most widely used superconducting materials like Nb–Ti and Nb_3Sn [4–8], a similarly robust process has not been successfully developed for the more recently discovered superconductor families [9]. MgB_2 is a promising technological superconducting material with a relatively high transition temperature, T_c, that is also much cheaper to manufacture in wire form than some of the materials with higher T_c values [2]. Epoch Wire Ltd employs a powder-in-tube (PIT) method for producing monofilament MgB_2 wire with capacity to produce long lengths of wire [10, 11].

Several studies have investigated the fabrication of joints for monofilament and multifilament MgB_2 wires [4–6, 12–16],

* Author to whom any correspondence should be addressed.

Table 1. Summary of performance of superconducting joints for reacted MgB_2 wires and tapes at 20 K in self-field. The decay measurements are calculated from the persistent current relative to the transport I_c of the wire.

Wire details	Transport measurements			Decay measurements			References
	Wire I_c	Joint I_c	CCR	R	I	CCR	
12-filament twisted reacted tape 0.65 × 3.65 mm	700 A	—	—	$<10^{-14}$ Ω	300 A	43%	[24]
Monofilament reacted round wire 2 mm ∅	—	51 A	—	—	—	—	[15]
19-filament reacted tape 0.71 × 3.10 mm	>300 A	>150 A	<50%	$<10^{-11}$ Ω	10 A	<4%	[25]

many of them concentrating on joining unreacted MgB_2 wires where the in-situ reaction to create the superconducting phase is carried out on the full wire and joint assembly—a *wind and react* strategy for complete magnet coils. Rather fewer reports have been published on joints between already reacted MgB_2 wires or windings [17–19], where the joints to complete the superconducting circuit can be made (or repaired) after the magnet has been fabricated by a *react and wind* process. One of the main reasons that this is more challenging is that the grain connectivity of ex-situ MgB_2 bulks and wires has been found to be inferior to that of in-situ fabricated MgB_2 samples due to weak intergranular coupling and impurities remaining between the MgB_2 grains even after sintering at high temperatures [20, 21].

There are two important figures of merit for assessing the performance of superconducting joints: (i) joint resistance measured from the magnetic field decay of a jointed coil, and (ii) the critical current ratio (CCR), which is defined as the ratio of the critical current of the joint compared to the critical current of the wire ($I_{c,joint}/I_{c,wire}$). Often $I_{c,joint}$ values are extracted from four-point transport I–V measurements, typically using a 1 μV cm^{-1} electric field criterion. Since this corresponds to a resistance value orders of magnitude higher than the resistance required for persistent currents, $I_{c,joint}$ values extracted from I/V measurements will overestimate the maximum persistent current that the joint can carry in a real magnet.

The first persistent joints for react and wind MgB_2 magnets were reported by ASG superconductors (Columbus) in 2007 [22]. They obtained a transport joint I_c value of 40 A at 20 K in self-field using monofilamentary Ni-sheathed wire, and estimated a joint resistance $<10^{-14}\,\Omega$ with an injected current of 30–40 A. Although details of the wire I_c was not given in the paper, a separate publication reported values of around 700 A at 20 K for this type of wire [23]. Therefore, we estimate the CCR of <6% for these preliminary joints. Nardelli *et al* published a follow-on study on the performance of coils made from 12-filament twisted reacted MgB_2 tapes, achieving much higher trapped currents of 300 A and 200 A for coils with one and two joints respectively, and resistances $<10^{-14}$ Ω under 20 K self-field [24]. The I_c value of the wire was estimated to be 700 A at 20 K, giving a CCR of ∼43% for the coil with one joint. However, no details are given in the literature on the ASG joint fabrication process. Luo *et al* [15] introduced a joint design utilizing the internal magnesium diffusion method for PIT processed reacted monofilamentary MgB_2 wires and achieved transport I_c values of 46 A and 51 A at 20 K and self-field after pressing at 940 MPa and 392 MPa, respectively. The CCR is unknown since the I_c of the wire was not given, but the T_c value across the joint was 39 K, close to the value in the wire. Mine *et al* [25] described a jointing strategy for reacted MgB_2 multifilamentary wires for their 3 T MRI magnet designed by general electric, consisting of six coils that required at least five joints to achieve persistent mode operation. A transport I_c value >150 A at 20 K in self-field was obtained on a test joint, but I_c dropped dramatically to <50 A in a field of 0.46 T. Since the I_c value of the wire was reported to be >300 A at 25 K, the CCR is estimated to be <50%. A joint resistance less than 10^{-11} Ω in a 14 turn, 300 mm diameter test coil was also measured using the much smaller current of 10 A. They pointed out that the joint performance they achieved was not yet adequate for adoption in real magnets as they were unable to achieve sufficient manufacturing consistency and noting that improvements in the jointing technology were still required.

Table 1 provides a summary of the performance of joints using reacted MgB_2 wires or tapes. The reported critical current ratios are quite low, with the joints, at best, carrying less than half the critical current of the wire. The size of the joint is another important design parameter for the magnet engineer that is typically not described in the literature. In this study, we present details of the processing, microstructure and performance of small termination joints specifically designed for PIT-processed reacted monofilament MgB_2 wire.

2. Experimental details

Both the MgB_2 wires and the joint are based on monocore production samples from Epoch Wires Ltd, and use a composite steel/Ti sheath design. To form the wires the sheath is filled with a mixture of magnesium powder (MGP-100/150 with average size between 100 and 150 μms from Almamet) and

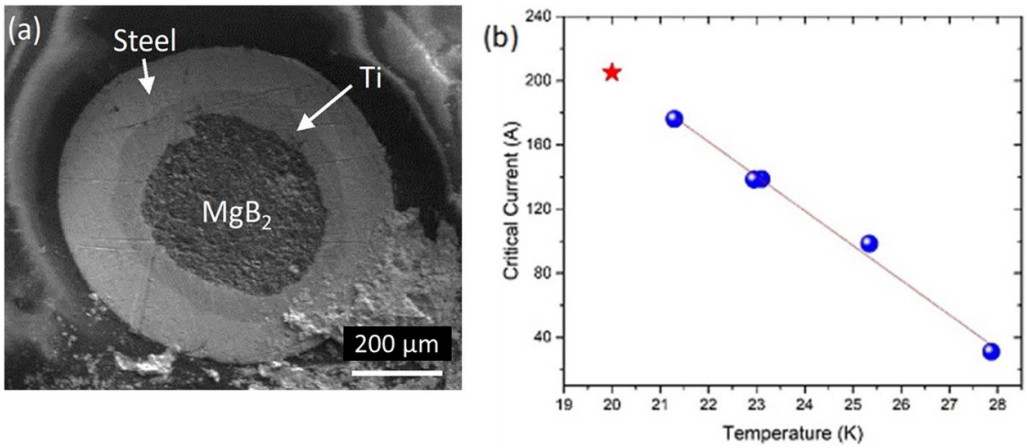

Figure 1. (a) SEM cross-sectional image of the reacted MgB_2 wire. (b) The temperature dependence of the critical current (I_c) for the wire in a 1 T background field. The extrapolated fit line allows an estimate of the I_c value at 20 K (represented by the star).

boron powder (PVZ Boron 95, amorphous boron powder 95% purity from PAVEZYUM) to form a monocore wire. After drawing, the external sheath has outer and inner (core) diameters of 0.75 mm and 0.38 mm, respectively, as shown in figure 1(a).

The critical current value of this wire, as a function of temperature under a background field of 1 T, is illustrated in figure 1(b). The I_c value below 20 K could not be obtained due to excessive heating of the copper wire that was used as a shunt. Based on the observed trend in the plot, an I_c value of 206 A for the wire at 20 K and 1 T has been estimated by linear extrapolation.

2.1. Joint fabrication process

Our strategy to form joints with the smallest possible volume involves using short lengths (20 mm) of a similar monocore wire at an earlier stage of the manufacturing process when the external diameter is still 5.5 mm. This joint piece (or *case* as it is referred to below) is already filled with unreacted Mg and B powders (magnesium powder atomised, D50, with average size 30 μms from SFM and same PVZ nano boron powder indicated above).

Figure 2(a) gives a schematic of the procedure we have designed to fabricate superconducting joints. All of these manufacturing processes were conducted under standard laboratory conditions. First the ends of the wires are polished diagonally on a workshop grinding wheel to increase the surface area of reacted MgB_2 in contact with Mg + B powders inside the case. During the coil production stage depicted in figure 4(a), the two upward-extending wire ends were ground using the same simple procedure. This scarf architecture has been shown by other authors to be an important factor in improving joint performance [26–28]. The case is then prepared to receive the ends of these two wires, first by smoothing the surface on one end of the 20 mm case with 400 mesh grinding paper and then by drilling two 9 mm holes into the unreacted powder filling the case. The ends of the two wires to be joined are then inserted into these holes (figure 2(b)), and 1.7 MPa pressure is applied laterally to the case for 10 min to ensure good contact of the ends of the reacted wires with the unreacted powder in the case. A conventional hydraulic pressing tool was used, with a known area of pressing die in contact with the joint, and the direction of the applied pressure is shown in figure 2(c).

No powder leakage was observed from the case during the pressing operation, and so we did not need to use any sealant.

The next stage is to heat treat the joint. The joint and the coil are separated by an alumina foam isolator, as shown in figure 3, to avoid over-reacting the already reacted wire wound on the former. Various one-step and two-step heat treatments at temperatures between 700 °C and 900 °C in flowing Ar have been explored, with the aims of obtaining high quality MgB_2 in both the wires and the joint itself, and good connectivity across the interface between the two regions.

2.2. Microstructural characterisation of joints

X-ray diffraction (XRD) analysis was carried out using a PANalytical Empyrean diffractometer with Cu K_α radiation generated at 40 kV and 40 mA. The spectra were analysed using Rietveld refinement in the PANalytical HighScore Plus programme. Scanning electron microscopy (SEM) was performed on a Zeiss EVO equipped with an Oxford Instruments X-act energy dispersive x-ray (EDX) detector. Joints were sectioned and polished using non-aqueous solutions prior to characterisation in the SEM. The EDX chemical composition data was analysed using Oxford Instruments Aztec software.

2.3. Transport measurements

In order to optimise the heat treatment protocol, prototype joints were fabricated using short, straight wires (instead of a coil) and tested using the conventional 4-point *I*–*V* method.

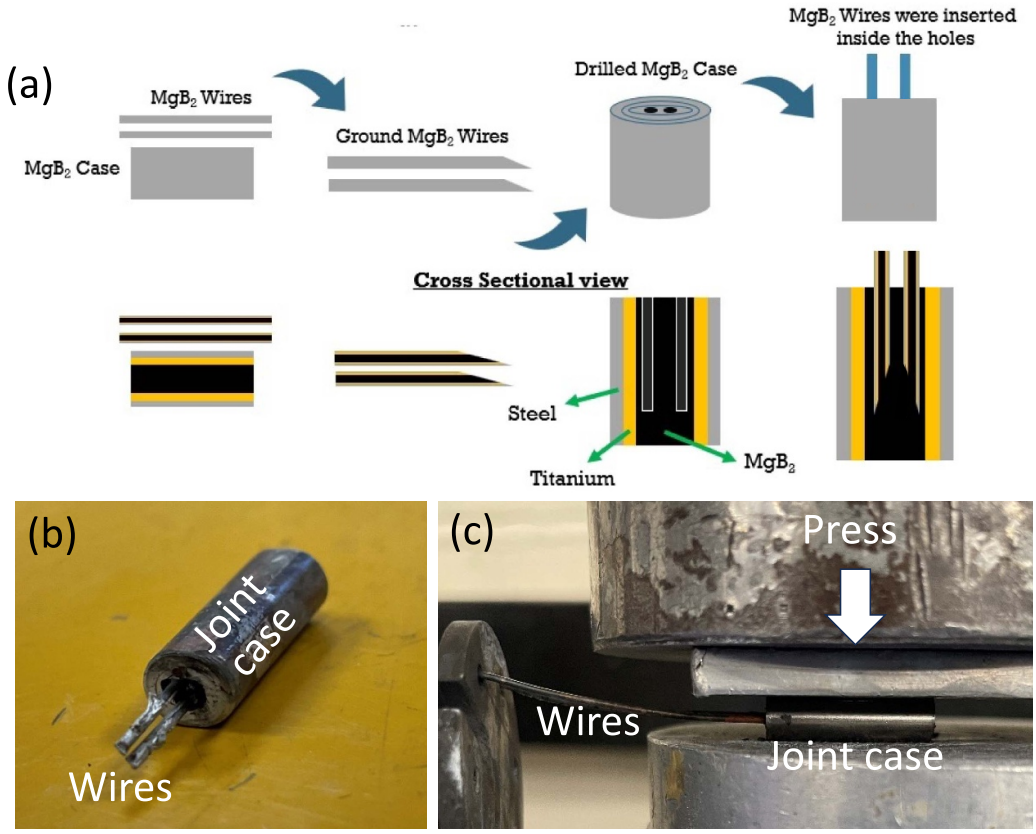

Figure 2. (a) Schematic illustration of the production processes for joints. (b) Photograph of a typical joint. The joint case is 20 mm long. (c) An illustration of the pressing operation applied to a joint.

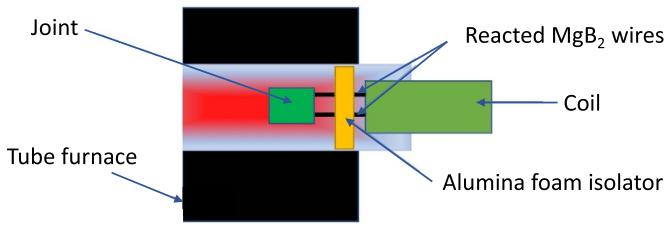

Figure 3. Schematic illustration of the joint heat treatment procedure.

voltage–current taps were connected using RS Pro silver conductive paste, and the joints inserted into a Model 22 CTI cryocooler. A DC current of 0.1 A was supplied by a keysight E36311A programmable DC Power Supply, and the voltage measured using a Keithley 2000 digital multimeter. To monitor the temperature, an SD706 silicon diode temperature sensor was positioned at the end of the probe, just above the sample. The samples were cooled to below the superconducting temperature and a LabView program recorded both voltage and temperature measurements during the natural, slow warming up phase after the cryocooler was switched off to minimise errors in the temperature measurements. Onset T_c values were extracted from the intersection of the tangent to the transition with a linear extrapolation of the normal state behaviour.

Table 2. Coil specifications. The inductance of these coils has been calculated using the long solenoid approximation.

Coil inner radius	r	6 mm
Coil outer radius	R	7 mm
Number of turns	N	29
Coil length	l	20 mm
Inductance	L	5.5×10^{-6} H

2.4. Inductive resistance testing (IRT)

IRT [29, 30] on an MgB_2 coil closed with a single joint has been used to measure the joint performance. Details of the coil specification are given in table 2. Since the minimum bending radius of these reacted MgB_2 wires is around 10 cm, to avoid severe degradation of performance, ∼1.3 m of unreacted MgB_2 wire was first wound onto the formers leaving the two ends extending outside the coil diameter as shown in figure 4(a). The coils were then reacted using the heat treatment developed by Epoch Wires: 700 °C for 15 min under an Ar atmosphere. This heat treatment results in wire with an I_c value of 206 A at 20 K and 1 T background field, as described above. An example of the final product can be seen in figure 4(b).

Figure 4(c) shows the basic layout of the measurement, carried out using a 9 T/3 T vector magnet in an Attodry cryostat.

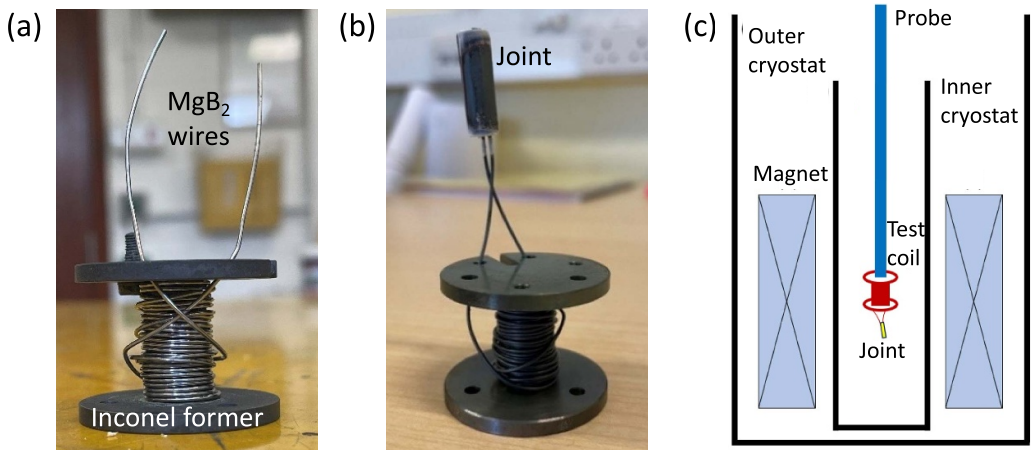

Figure 4. (a) MgB_2 coil prior to first heat treatment (700 °C for 15 min). (b) Jointed MgB_2 coil. (c) Schematic of the essential components of the IRT experimental set up showing the inner and outer cryostats, the background field magnet, and the experimental probe, which has magnetic field sensor (usually a Hall probe) at the tip, inserted in the middle of the jointed test coil.

The thermocouple employed for temperature monitoring was located as near as possible to the test coil, at the very bottom of the experimental probe. A Lakeshore HGT-2101 Hall probe was positioned at the centre of the test coil. To perform an IRT measurement, the external magnet is used to apply a field parallel to the axis of the coil. In a typical experiment, the applied field is increased to a maximum field, for instance 1.5 T, before being lowered (usually at a slower rate to avoid coil instability causing flux jumps) back to zero, or a desired background field, typically 1 T. We have calculated that during the measurements without applied background field, the self-field from the trapped current in the field at the location of the joints shown in figure 4 is only approximately 3 mT. Because the MgB_2 wire is monocore, the flux jumping behaviour becomes very severe at lower temperatures [31, 32], and so here we report results from experiments at 20 K.

To obtain the relation between circulating current (I) and trapped field (B), the following equation was derived from the Biot-Savart law, using the geometry and parameters of the test coils given in table 2:

$$I = \frac{B\sqrt{4r^2 + l^2}}{\mu_0 N} \tag{1}$$

where μ_0 is the vacuum magnetic permeability.

The decay of the trapped field can be described by:

$$B(t) = B_0 e^{\left(\frac{-R}{L}\right)t} \tag{2}$$

where B_0 is the initially induced magnetic field, R is the joint resistance and L is the coil inductance. This allows the extraction of joint resistance from the decay curve, with a value below $10^{-12}\Omega$ meeting the specification for persistent-mode magnets [33].

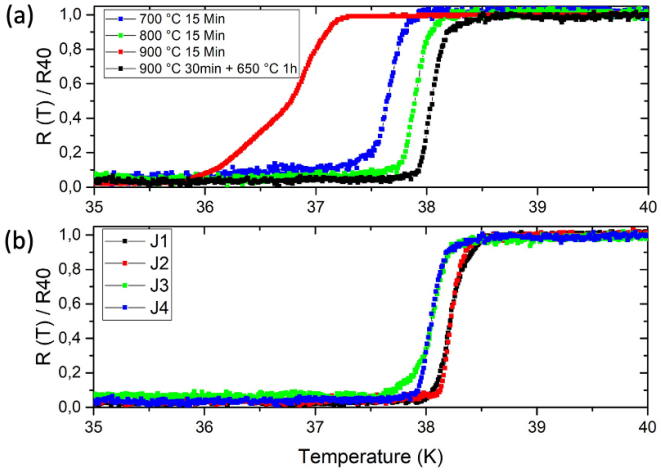

Figure 5. (a) R/T data for joints processed at different temperatures, and (b) the performance of 4 nominally identical joints processed by the two-step heat treatment process.

3. Results and discussion

3.1. Transport measurements

Low current measurements of resistance as a function of temperature on test joints made using short straight lengths of wire are presented in figure 5. Figure 5(a) compares the performance of joints prepared with single heat treatments at 700 °C, 800 °C, and 900 °C, and then after a two-stage heat treatment at 900 °C and then 650 °C. The joint fabricated at 700 °C has an onset T_c value of 37.8 K and a relatively wide transition, with a considerable tail before zero resistance is reached. Both T_c and the sharpness of the transition improve when the joint is heat treated at 800 °C, presumably because the higher reaction temperature results in improved stoichiometry and/or less disorder in the MgB_2 lattice, as well as improved homogeneity of the material through which the current passes. Increasing the

Table 3. Summary of the heat treatment steps and expected reactions, based on the literature [34, 35].

Heat treatment	First 700 °C 15 min	Second 900 °C 30 min	Third 650 °C 1 h
Wire	$Mg + B \rightarrow MgB_2$	$2MgB_2 \rightarrow MgB_4 + Mg$	$MgB_4 + Mg \rightarrow 2MgB_2$
Joint case	—	$Mg + B \rightarrow MgB_2$ $2MgB_2 \rightarrow MgB_4 + Mg$	$MgB_4 + Mg \rightarrow 2MgB_2$

temperature further to 900 °C leads to a substantial degradation in the performance of the joint. This is presumably as a result of the well-known thermal decomposition of MgB_2 to non-superconducting MgB_4 and Mg vapour that is expected to take place at this high temperature under ambient pressure [28]. However, an additional 650 °C heat treatment is found to dramatically improve the superconducting properties of joints reacted initially at 900 °C because the decomposition reaction can be reversed by annealing at lower temperature [29]. Detailed phase analysis to confirm this has been performed, and is reported and discussed in section B. Since the two-stage heat treatment at 900 °C followed by 650 °C results in the sharpest superconducting transition and the highest T_c value of 38.2 K, we have selected these conditions for our jointed coils.

To analyse the reproducibility of the process, R/T curves for four nominally identical samples ($J1$, $J2$, $J3$ and $J4$) were measured using a current of 0.1 A and self-field after the two-stage heat treatment, and the results shown in figure 5(b). All four have very similar T_c values (onset values between 38.2 K and 37.4 K), and although sample $J3$ has a slightly wider transition than the other three samples, suggesting the MgB_2 forming the continuous path may be more inhomogeneous, there is no evidence of any ohmic series resistance below the transition in any of the samples. This demonstrates that the joint preparation process reproducibly achieves a continuous superconducting pathway from one wire to the other through the joint, capable of carrying at least the low current of 0.1 A used in these measurements.

3.2. *Phase evolution during heat treatment*

In the manufacture of jointed coils, pre-reacted MgB_2 in the wires and Mg + B powders in the joint case are exposed to a series of heat treatments, as detailed in table 3. The wire undergoes three distinct thermal treatment steps: 700 °C for 15 min on its own, and then 900 °C for 30 min and 650 °C for 1 h during the jointing process. On the other hand, the Mg + B powders in the case are subjected to only two thermal treatment steps: 900 °C for 30 min and 650 °C for 1 h. The reasoning for choosing this multistage process has been described above, and the expected reactions in each stage are given in table 3. To investigate the extent of the phase evolution during these different thermal processing stages, five separate sections of the Mg + B filled joint cases (2 cm in length and 5.5 mm in diameter) were subjected to different heat treatment procedures, and the resulting reacted material extracted for XRD analysis.

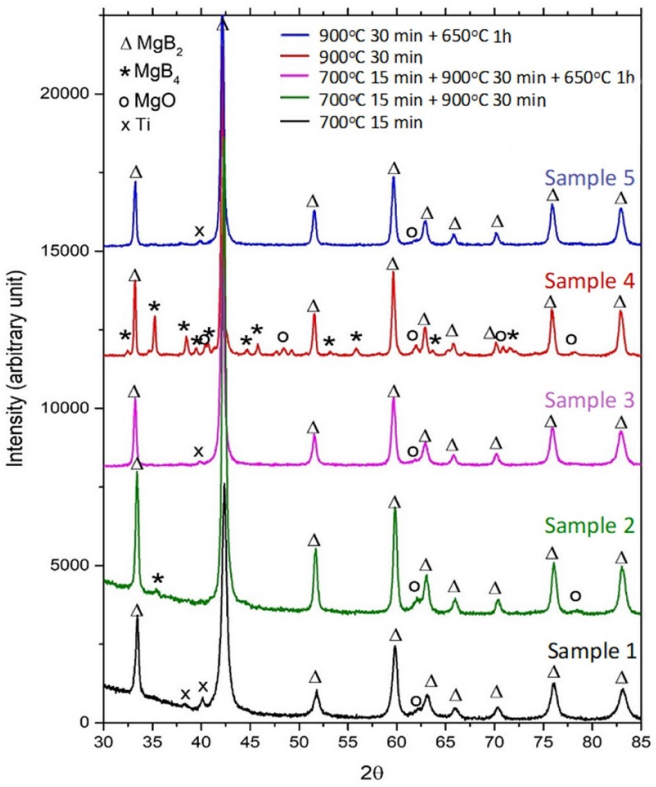

Figure 6. X-ray diffraction patterns of material formed in the case after heat treatments at different temperatures.

The details of the heat treatment procedures and the weight fractions of different phases determined from Rietveld refinement of the XRD patterns shown in figure 6, are given in table 4. The heat treatments received by samples 1, 2 and 3 mimic those experienced by the MgB_2 wires during the different stages of the manufacture of the jointed coil, whereas samples 4 and 5 give information about the phases formed within the joint at each step in the thermal treatment.

The results from sample 1 shows that the initial in situ wire reaction heat treatment at 700 °C for 15 min produces a high MgB_2 fraction, with a small amount of MgO. An additional thermal treatment at 900 °C for 30 min (sample 2) results in a slight increase in the fraction of MgO, along with the appearance of a small amount of MgB_4. This is consistent with a small fraction of the existing MgB_2 partially decomposing into MgB_4 and Mg vapour, as expected at this temperature, with the vaporized Mg reacting with adventitious oxygen to produce MgO. In contrast, the results from sample 4 show that performing the reaction between Mg and B at the higher temperature of 900 °C, without the prior 700 °C stage, leads

Table 4. The phase fractions in the wire core and the case after each heat treatment step.

Sample number	Heat treatment	Weight fraction (%)				Received by
		MgB_2	MgB_4	MgO	Ti	
1	700 °C 15 min	99.4	—	<1	Trace	Wires
2	700 °C 15 min + 900 °C 30 min	98.1	<1	1.4	—	Wires in joint
3	700 °C 15 min + 900 °C 30 min + 650 °C 1 h	99.0	—	<1	Trace	Wires in joint
4	900 °C 30 min	68.9	29.6	1.5	—	Joint filler
5	900 °C 30 min + 650 °C 1 h	98.9	—	<1	Trace	Joint filler

to the formation of a considerably higher fraction of MgB_4. However, subjecting the samples heat treated at 900 °C to a subsequent anneal at 650 °C (samples 3 and 5) successfully transforms nearly all of the MgB_4 back to MgB_2. This suggests that the Mg vapour released during the in-situ reaction of Mg and B at 900 °C does not escape from the joint case completely. In some of the samples, a trace amount of Ti was also detected. This contamination is likely to have arisen when the reacted material was extracted from the Ti sheath. The MgO fraction in sample 5 appears surprisingly to be slightly lower than in sample 4, but the difference is within the expected sample to sample variation. The most important point is that there is little evidence that a large volume fraction of MgO is produced during the joint making process, which might result in insulating phases in the joint region.

These XRD results suggest that at the end of the two-stage joint-making process, we would expect to obtain a high fraction (>98%) of the superconducting MgB_2 phase in both components of the joint. To confirm this, SEM/EDX analysis was performed on a polished section through a typical joint that had undergone the full heat treatment protocol. As can be observed in figure 7, the microstructure of the MgB_2 in the wire and case regions are very different as they have been formed by reactions at different temperatures, but the MgB_2 phase forms a continuous path across the interface between the wire and the joint filler material within the case, without any evidence of pores or cracks. The oxygen map shows that a significant volume fraction of MgO is formed in both regions. This can be attributed both to the trapping of air in the joint during pressing and the exposure of the polished surface to air before analysis. In addition, a small number of Ti and Fe counts can be seen within the MgB_2 of the wire and joint. This is likely to be a result of transfer of the relatively soft metals from the sheath into the pores in the MgB_2 during polishing.

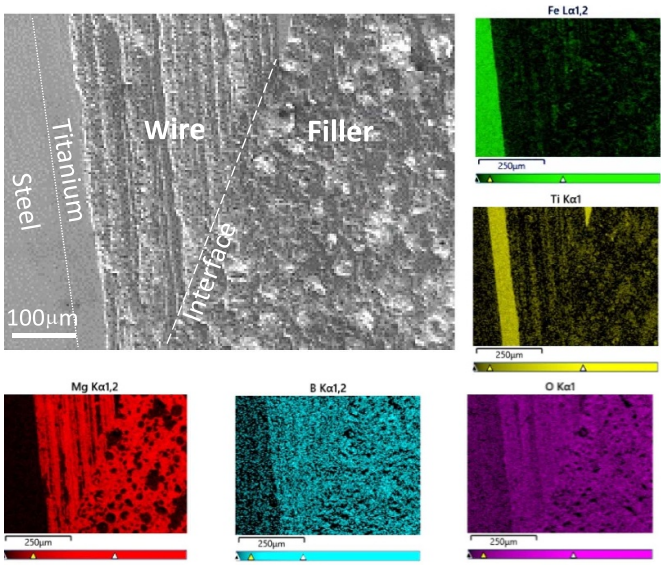

Figure 7. SEM image and elemental distributions at the interface between the MgB_2 wire filament and the MgB_2 formed in the joint case during the heat treatment. The dashed line marks the position of the original polished end of the wire.

3.3. Field decay measurements

The IRT field decay technique was used to characterise the persistent-mode characteristics of the joints. Figure 8(a) shows a typical energisation profile of a 1 T background field measurement, where a maximum field of 1.4 T was applied to energise the coil. The ramp down rate was significantly slower than the ramp up rate to prevent the effects of flux jumping due to the unstable nature of the monocore wire. Figures 8(b)–(d) show typical persistent mode performance of a coil at 20 K in 1 T background field (b) and in self field (c).

The trapped fields stabilised at 0.27 T and 0.25 T in self-field and 1 T background field respectively, corresponding to trapped currents of 172 A and 160 A, and the resistance in both cases was below 10^{-12} Ω (see the curves in supplementary data, figure S1), clearly satisfying the persistence criterion. The calculated resistance after settling, using equation (2), for the self-field and 1 T decay was 5.5×10^{-14} Ω and 5.6×10^{-14} Ω respectively. The currents correspond to a CCR of 78% at 20 K in a 1 T background field, based on a wire I_c of 206 A (figure 1). Since the wire I_c is not known under self-field conditions, the CCR value in zero background field cannot be calculated. We repeated the energisation process multiple times and find that the coil can be warmed and cooled and re-energised without any signs of performance degradation. In the supplementary data, figure S2, we show a second energisation with a very similar performance.

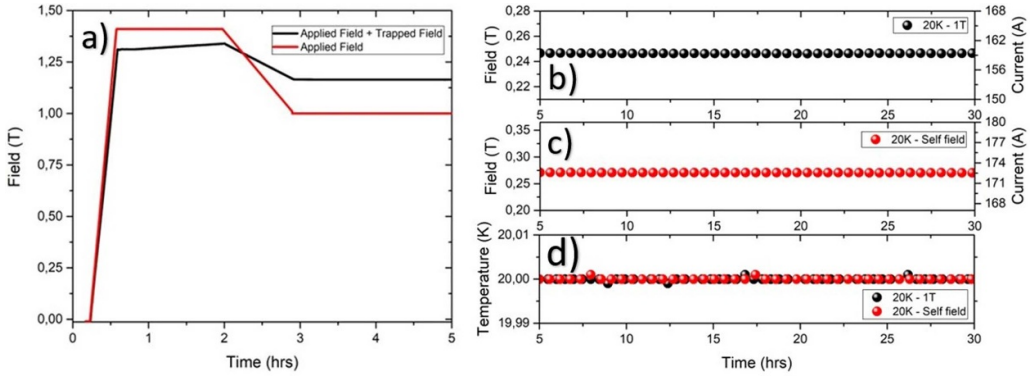

Figure 8. (a) A typical energisation profile of a 1 T background field experiment. Measured field and current calculated of the closed coil from using equation (1) given in the method at (b) 20 K and 1 T field, (c) 20 K and self-field. and (d) the logged temperature during the measurement. data in (b) and (c) has been binned and the raw data in included in supplementary materials.

4. Conclusions

We have demonstrated a simple process for introducing persistent joints into monofilament reacted MgB_2 wires. The key stages of the joining process include inserting reacted monofilament wires into pre-drilled holes in unreacted Mg + B powder in a joint case, and a pressing operation designed to place the exposed wire ends into close mechanical contact with the powder, before a final two-step heat treatment process designed to achieve good density and connectivity and a low fraction of non-superconducting impurity phases. We have also shown that this joint fabrication method resulted in a well-connected interface between wire and joint filler, and as a result, residual resistances below 10^{-12} Ω were achieved. Trapped persistent currents of 172 A and 160 A were obtained in self-field and 1 T background field, respectively. The CCR has been calculated as 78% under a 1 T background field at a temperature of 20 K, which is the highest value reported to date for joints made between reacted MgB_2 wires. These results suggest that a robust jointing process, suitable for the manufacturing of persistent mode *react and wind* MgB_2 magnets at operating temperatures at least as high as 20 K can be achieved.

Data availability statement

The data that support the findings of this study are openly available at the following URL/DOI: https://github.com/muslumguvenn/Persistent-MgB2-joints-for-react-and-wind-magnets and https://ora.ox.ac.uk/objects/uuid:1bce4a03-bd42-44e3-9e85-5947f876fd0b .

Acknowledgments

This study received financial support from the Ministry of National Education, Republic of Turkey.

Furthermore, the authors acknowledge use of characterisation facilities within the David Cockayne Centre for Electron Microscopy, Department of Materials, University of Oxford, alongside financial support provided by the Henry Royce Institute (Grant ref EP/R010145/1)

ORCID iDs

M Guven https://orcid.org/0000-0001-6196-5007
P Zagura https://orcid.org/0009-0004-6194-394X
C M Barker https://orcid.org/0000-0001-5710-9363
C R M Grovenor https://orcid.org/0000-0001-6425-354X
S C Speller https://orcid.org/0000-0002-6497-5996

References

[1] Baig T *et al* 2017 Conceptual designs of conduction cooled MgB_2 magnets for 1.5 and 3.0 T full body MRI systems *Supercond. Sci. Technol.* **30** 043002
[2] Parizh M, Lvovsky Y and Sumption M 2017 Conductors for commercial MRI magnets beyond NbTi: requirements and challenges *Supercond. Sci. Technol.* **30** 014007
[3] Patel D *et al* 2016 Evaluation of persistent-mode operation in a superconducting MgB_2 coil in solid nitrogen *Supercond. Sci. Technol.* **29** 04LT02
[4] Cheng J *et al* 2012 Fabrication of NbTi Superconducting Joints for 400-MHz NMR application *IEEE Trans. Appl. Supercond.* **22** 4300205
[5] Fukuzaki T, Maeda H, Matsumoto S, Nimori S, Yokoyama S and Kiyoshi T 2006 Development of a superconducting joint for high field NMR *IEEE Trans. Appl. Supercond.* **16** 1547–9
[6] Liu S, Jiang X, Chai G and Chen J 2013 Superconducting joint and persistent current switch for a 7-T animal MRI magnet *IEEE Trans. Appl. Supercond.* **23** 2–5
[7] Patel D, Kim S-H, Qiu W, Maeda M, Matsumoto A, Nishijima G, Kumakura H, Choi S and Kim J H 2019 Niobium-titanium (Nb-Ti) superconducting joints for persistent-mode operation *Sci. Rep.* **9** 14287
[8] Swenson C A and Denis Markiewicz W 1999 Persistent joint development for high field NMR *IEEE Trans. Appl. Supercond.* **9** 185–8
[9] Cardwell D A, Larbalestier D C and Braginski A I 2021 E5.3 persistent mode joints *Handbook of Superconductivity—Processing and Cryogenics* 2nd edn vol II (Taylor and Francis Group) pp 480–92
[10] Kutukcu M N, Atamert S, Scandella J-L, Hopstock R, Blackwood A C, Dhulst C, Mestdagh J, Nijhuis A and Glowacki B A 2018 Composite superconducting MgB_2

wires made by continuous process *IEEE Trans. Appl. Supercond.* **28** 1–4
[11] Atamert S, Kutukcu M N, Scandella J L, Baskys A, Zhong Z and Glowacki B A 2016 Novel superconducting MgB_2 wires made by continuous process *IEEE Trans. Appl. Supercond.* **26** 1–4
[12] Valente-Feliciano A M 2016 Superconducting RF materials other than bulk niobium: a review *Supercond. Sci. Technol.* **29** 113002
[13] Wózniak M, Glowacki B A, Setiadinata S B and Thomas A M 2013 Pulsed magnetic field assisted technique for joining MgB_2 conductors for persistent mode MRI magnets *IEEE Trans. Appl. Supercond.* **23** 6200104
[14] Giunchi G, Saglietti L, Ripamonti G, Albisetti A F, Bassani E and Perini E 2010 Superconducting joints between MgB_2 wires and bulks *IEEE Trans. Appl. Supercond.* **20** 1524–7
[15] Luo W *et al* 2019 MgB_2 superconducting joint technique based on Mg diffusion method *IEEE Trans. Appl. Supercond.* **29** 1–5
[16] Patel D *et al* 2021 Superconducting joining concept for internal magnesium diffusion-processed magnesium diboride wires *ACS Appl. Mater. Interfaces* **13** 3349–57
[17] Li X H, Ye L Y, Jin M J, Du X J, Gao Z S, Zhang Z C, Kong L Q, Yang X L, Xiao L Y and Ma Y W 2008 High critical current joint of MgB_2 tapes using Mg and B powder mixture as flux *Supercond. Sci. Technol.* **21** 025017
[18] Li X, Ye L, Zhang D, Wang D and Ma Y 2010 Joints in MgB2 tapes and wires for persistent current operating magnet *IEEE Trans. Appl. Supercond.* **20** 1528–31
[19] Li X *et al* 2011 A small 1.5 T persistent current operating test magnet using MgB_2 wire with high jc joints *IEEE Trans. Appl. Supercond.* **21** 1616–9
[20] Yamamoto A, Tanaka H, Shimoyama J I, Ogino H, Kishio K and Matsushita T 2012 Towards the realization of higher connectivity in MgB_2 conductors: in-situ or sintered ex-situ? *Jpn. J. Appl. Phys.* **51** 010105
[21] Dancer C E J, Mikheenko P, Bevan A, Abell J S, Todd R I and Grovenor C R M 2009 A study of the sintering behaviour of magnesium diboride *J. Eur. Ceram. Soc.* **29** 1817–24
[22] Braccini V, Nardelli D, Penco R and Grasso G 2007 Development of ex situ processed MgB_2 wires and their applications to magnets *Physica* C **456** 209–17
[23] Grasso G *et al* 2004 Present status and future perspectives for Ni-sheathed MgB_2 superconducting tapes *Inst. Phys. Conf. Ser.* **181** 45–52
[24] Nardelli D, Angius S, Capelluto A, Damiani D, Marabotto R, Modica M, Perrella M and Tassisto M 2010 Persistent mode MgB_2 short windings *IEEE Trans. Appl. Supercond.* **20** 1998–2001
[25] Mine S, Xu M, Bai Y, Buresh S, Stautner W, Immer C, Laskaris E T and Amm K 2015 Development of a 3 T—250 mm bore MgB_2 magnet system *IEEE Trans. Appl. Supercond.* **25** 12–15
[26] Patel D, Al Hossain M S, Wai See K, Xu X, Barua S, Ma Z, Choi S, Tomsic M and Ho Kim J 2015 MgB_2 superconducting joints for persistent current operation *Supercond. Sci. Technol.* **28** 065017
[27] Patel D, Matsumoto A, Kumakura H, Nishijima G, Maeda M, Kim S-H, Choi S and Kim J H 2020 Tailored joint fabrication process derived ultra-low resistance MgB_2 superconducting joint *Scr. Mater.* **178** 198–202
[28] Patel D, Matsumoto A, Kumakura H, Maeda M, Kim S-H, Liang H, Yamauchi Y, Choi S, Kim J H and Hossain M A 2021 Superconducting joints using multifilament MgB_2 wires for MRI application *Scr. Mater.* **204** 114156
[29] Brittles G D, Mousavi T, Grovenor C R M, Aksoy C and Speller S C 2015 Persistent current joints between technological superconductors *Supercond. Sci. Technol.* **28** 093001
[30] Leupold M J and Iwasa Y 1976 Superconducting joint between multifilamentary wires 1. Joint-making and joint results *Cryogenics* **16** 215–6
[31] Wang X L, Soltanian S, Horvat J, Liu A H, Qin M J, Liu H K and Dou S X 2001 Very fast formation of superconducting MgB2/Fe wires with high Jc *Physica* C **361** 149–55
[32] Pan A V, Zhou S, Liu H and Dou S 2003 Properties of superconducting MgB_2 wires: in situ versus ex situ reaction technique *Supercond. Sci. Technol.* **16** 639
[33] Lakrimi M *et al* 2011 The principles and evolution of magnetic resonance imaging *J. Phys.: Conf. Ser.* **286** 012016
[34] Fan Z Y, Hinks D G, Newman N and Rowell J M 2001 Experimental study of MgB_2 decomposition *Appl. Phys. Lett.* **79** 87–89
[35] Peng J, Cai Q, Cheng F, Ma Z, Li C, Xin Y and Liu Y 2017 Enhancement of critical current density by a 'MgB2-MgB4′ reversible reaction in self-sintered ex-situ MgB_2bulks *J. Alloys Compd.* **694** 24–29